Rapid communication

Ion beam smoothing of indium-containing III-V compound semiconductors

F. Frost, A. Schindler, F. Bigl

Institute for Surface Modification, Permoserstrasse 15, D-04318 Leipzig, Germany
(Fax: +49-341/235-2595, E-mail: ffrost@server1.rz.uni-leipzig.de)

Abstract. Reactive ion beam etching (RIBE) with N_2 has been used for smoothing of rough InAs, InP, and InSb surfaces, prepared by argon ion beam etching (IBE). The evolution of the surface roughness and morphology has been studied by atomic force microscopy (AFM) as a function of the N_2 RIBE process parameters (ion beam energy, ion beam angle of incidence, and ion dose). A drastic improvement of the surface roughness has been observed for ion beam angles near normal incidence and larger than 70° with increasing ion doses. By using this technique, the initial root-mean-square (rms) roughness of, e.g., InSb of about 40 nm could be decreased to about 1 nm.

PACS: 52.75.Rx; 81.65.Cf; 61.16.Ch

The indium-containing semiconductors InP, InAs, and InSb play an important role for a lot of potential applications in photonic and electronic devices. Their electronic characteristics make these materials attractive for modern telecommunication systems (InP), infrared detectors and emitters (InAs, InSb), and high-speed electronic devices. Therefore, the study of these materials is attracting a wide attention.

It is well known that the roughness of the etched surfaces is very important for the operation and quality of optical components (laser mirror facets) and electronic devices. In comparison to Ga-based semiconductors, where inert IBE with argon has been successfully used for dry etching, sample preparation for transmission electron microscopy (TEM), and depth profiling with Auger electron spectroscopy (AES) or secondary ion mass spectrometry (SIMS), Ar IBE was not suitable for indium-containing semiconductors. This is because InP, InAs, and InSb have proven to be very susceptible to roughness development during argon ion beam etching or sputtering [1–7]. For InP it has been proposed that indium enrichment, due to the preferential sputtering of phosphor, and the surface diffussion of indium are the main mechanisms for the roughness evolution [8]. As a result of the different etch rates of indium and the surrounding InP, the indium islands act as seeding points for the cone (and hence roughness) evolution during the sputtering process [8].

Recently it has been demonstrated that reactive gases or gas mixtures such as Ar/O_2 [1] and I_2 [9] can be used to overcome this problem. The utilization of N_2 or N_2/O_2 for reactive ion beam etching (RIBE) in particular results in very smooth and less-damaged surfaces on InP [10–13]. This method also reveals extremly smooth surfaces on InAs and InSb [7].

In this study, the smoothing of InP, InAs, and InSb surfaces by N_2 reactive ion beam etching is demonstrated. The preparation of rough surfaces, as the starting point for the ion beam smoothing, was done by Ar IBE. By changing the ion dose, this process can be used to prepare surfaces with different rms surface roughness [5–7]. The only reason we used Ar IBE for the preparation of rough surfaces was to have a procedure that allows the reproducible preparation of well-defined rough surfaces and hence a detailed investigation of the smoothing process. Generally one can start with arbitrarily rough surfaces that require smoothing.

The influence of the N_2 RIBE process parameters (ion beam energy E_{ion}, ion beam angle of incidence α_{ion}, and ion dose D_{ion}) on the evolution of the surface roughness and morphology have been examined by using atomic force microscopy. To the best of our knowledge this is the first study to report on smoothing of In-containing semiconductor surfaces by ion beam etching.

1 Experimental details

The samples used in this work were commercially available nominally undoped Czochralski-grown (100) InAs and (100) InSb substrates ($n \approx 1.5 \times 10^{16}$ cm^{-3} and $n \leq 2 \times 10^{14}$ cm^{-3}, respectively). The (100) InP substrates were semi-insulating (Fe-doped) material. Ion beam etching was performed in a Hochvakuum Dresden model ISA 150 ion beam etching system with a Kaufman-type graphite lining source and a beam diameter of 15 cm. The positive Ar or N_2 ion beam was neutralized with thermal electrons produced by a neutralizer filament between the source and the substrate holder to prevent the charge accumulation on the substrate. The ion current was measured by a Faraday cup without neutralization and the water-cooled substrate stage was rotated during the

etching process. The angle of ion beam incidence was varied between 0° an 80° to the surface normal. The vacuum chamber was pumped by a turbopump to a base pressure of 1×10^{-6} mbar. The chamber pressure during etching was set by the total gas flow rate (controlled by a MKS flow control system). The gas flow was adjusted to 2.5 standard cubic centimetres per minute (sccm) for Ar IBE and 3.5 sccm for N_2 RIBE, respectively. All experiments were carried out with an ion beam current density of 200 μA cm^{-2}.

The morphology of the ion beam etched surfaces was investigated by atomic force microscopy by using a Nanoscope III from Digital Instruments working with silicon tips. All measurements were conducted in air and in contact mode. To quantify the surface roughness we used the arithmetical average of the rms roughness R_q of typically three or more scans $(10 \times 10\, \mu m^2$ or $3 \times 3\, \mu m^2)$ on different positions of the sample. Furthermore, we analyzed the surfaces by using the power spectral density (PSD) function, because this spectral analysis is more informative than the commonly used statistical quantities (R_q). The PSD function reveals periodic surface features and provides a measure of how such features are distributed (i.e. which wavelength occur most often and which has the greatest influence on the surface morphology) [14–17].

2 Results and discussion

The preparation of different rms roughness values on the semiconductor surfaces was done by Ar ion beam etching. We used as standard process parameters an Ar ion energy of 500 eV, an ion current density of 200 μA cm^{-2}, and an angle of ion beam incidence of 0°. The rms roughness is a function of the ion dose. With increasing ion dose the roughness of surface is enlarged [5–7].

Three typical surfaces, used as the starting point for the ion beam smoothing, are illustrated in Figs. 1a, 2a and 3a. The InSb, InP, and InAs samples have initial rms roughness values of $R_q = (36.5 \pm 4.5)$ nm, $R_q = (3.3 \pm 1.1)$ nm, and $R_q = (2.8 \pm 0.1)$ nm, respectively. All surfaces show the characteristic cone-like structure that is typical for Ar ion beam etched surfaces of indium-containing semiconductor material surfaces [5–7]. It should be mentioned here that the z scale of all the AFM images was intentionally expanded in order to clarify the topography characteristics. After N_2 RIBE with $E_{ion} = 200$ eV, $\alpha_{ion} = 0°$, and an ion dose of $D_{ion} = 1.8 \times 10^{19}$ cm^{-2}, the surface roughness for all three samples has been extremely improved, as shown in Figs. 1b, 2b and 3b. The rms surface roughness values are reduced to $R_q = (1.4 \pm 0.1)$ nm, $R_q = (0.8 \pm 0.1)$ nm, and
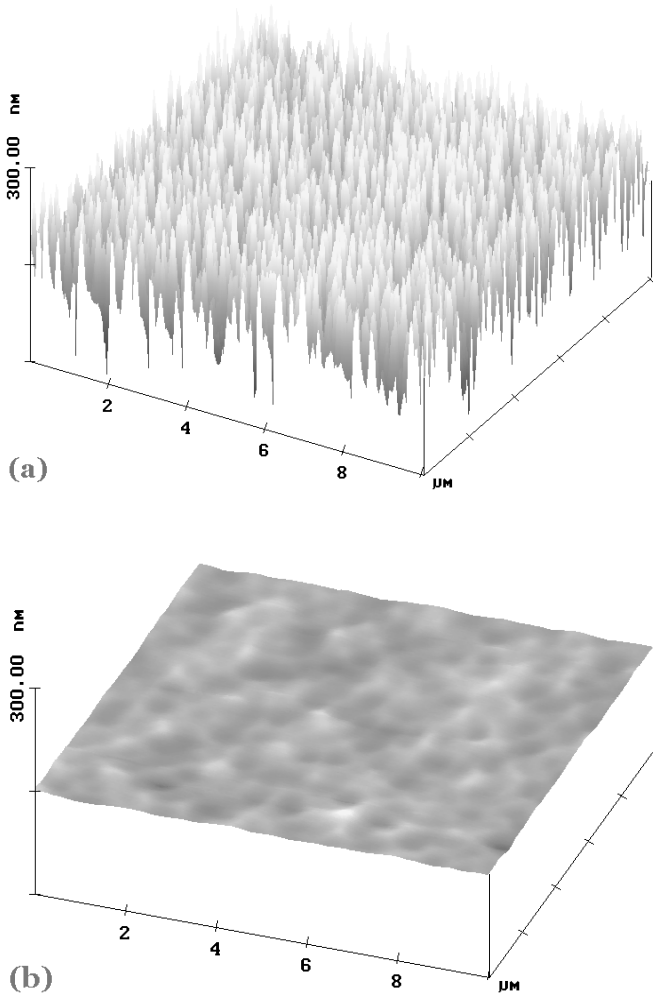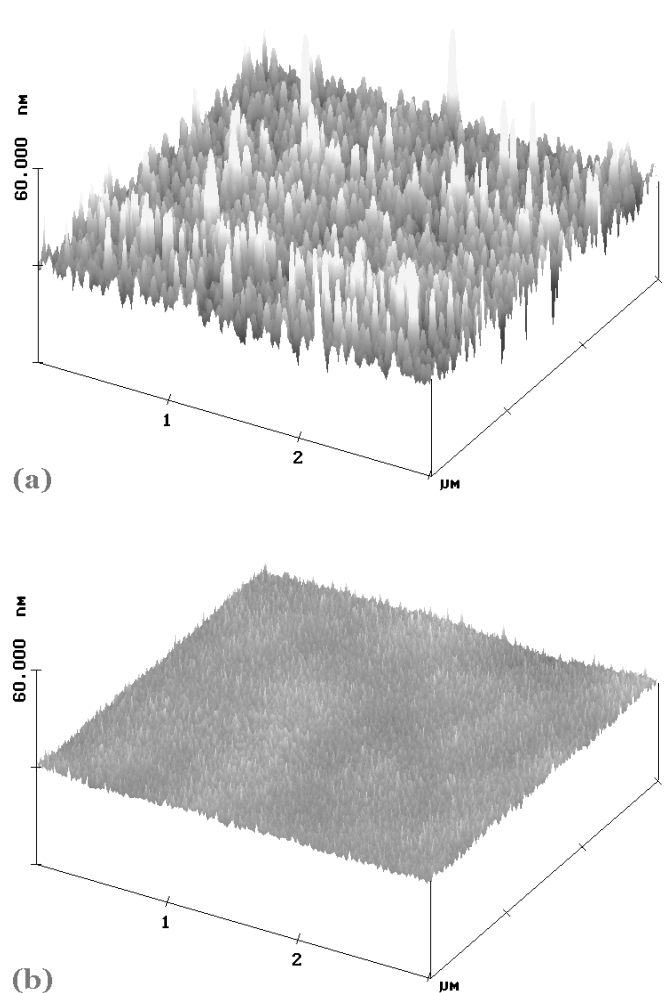

Fig. 1a,b. AFM images of the InSb surface: **a** before ion beam smoothing and **b** after ion beam smoothing with N_2 at normal ion beam incidence $\alpha_{ion} = 0°$, ion energy $E_{ion} = 200$ eV and ion dose $D_{ion} = 1.8 \times 10^{19}$ cm^{-2}

Fig. 2a,b. AFM images of the InP surface: **a** before ion beam smoothing and **b** after ion beam smoothing with N_2 at normal ion beam incidence $\alpha_{ion} = 0°$, ion energy $E_{ion} = 200$ eV and ion dose $D_{ion} = 1.8 \times 10^{19}$ cm^{-2}
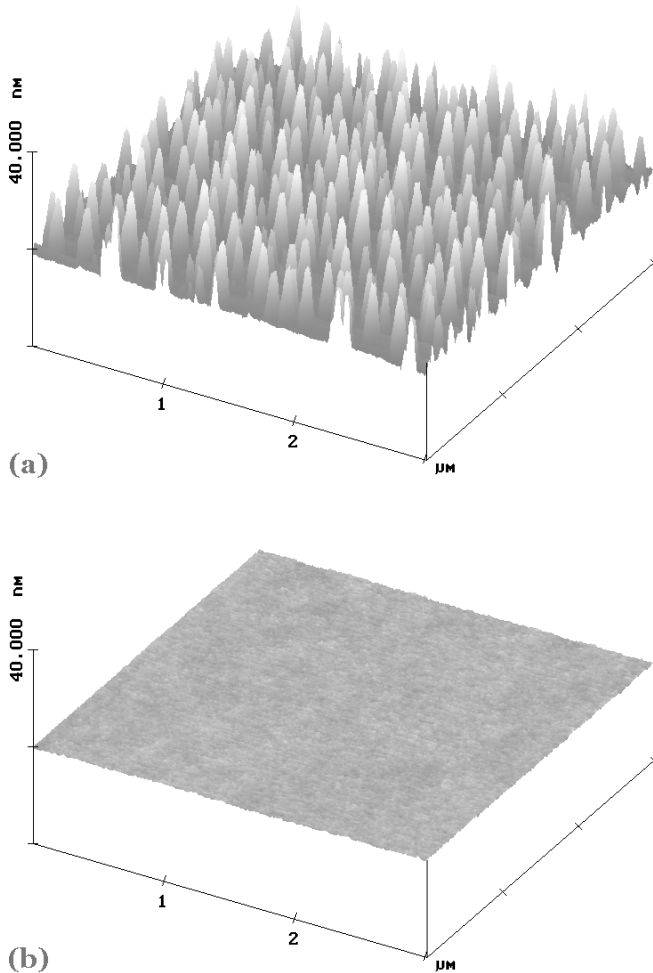
(a)

(b)

Fig. 3a,b. AFM images of the InAs surface: **a** before ion beam smoothing and **b** after ion beam smoothing with N_2 at ion beam normal incidence $\alpha_{\mathrm{ion}} = 0°$, ion energy $E_{\mathrm{ion}} = 200$ eV and ion dose $D_{\mathrm{ion}} = 1.8 \times 10^{19}$ cm^{-2}

Fig. 4. Evolution of rms surface roughness of InSb as a function of ion dose at two ion beam energies ($E_{\mathrm{ion}} = 200$ eV and $E_{\mathrm{ion}} = 500$ eV) for normal ion beam incidence

$R_q = (0.2 \pm 0.1)$ nm for the InSb, InP, and InAs samples, respectively. The etch rates under these N_2 RIBE conditions are 23 nm min^{-1} (InP), 19 nm min^{-1} (InSb), and 18 nm min^{-1} (InAs). The resulting roughness reduction as a function of the ion dose for the InSb and InP samples are shown in Figs. 4 and 5 for normal ion beam incidence at two ion beam energies ($E_{\mathrm{ion}} = 200$ eV and $E_{\mathrm{ion}} = 500$ eV). InAs (not illustrated) shows nearly the same behaviour as InSb. In principle all three materials show similar behaviour in the roughness reduction with ion dose. At first, for an ion dose less than 2.5×10^{18} cm^{-2} the rms surface roughness rapidly decreases. However, for ion doses $D_{\mathrm{ion}} > 2.5 \times 10^{18}$ cm^{-2} only a small improvement in the surface roughness can be observed. It is interesting to note that the same behaviour was observed for ion beam smoothing of thin diamond films at grazing incidence [18] and H^+ ion bombardment of initially rough SiO_2 surfaces [19, 20]. It must be mentioned here that the time necessary for sufficient smoothing depends both on the initial roughness of the surfaces and on the current density of the etching process. Generally the smoothing time can be reduced for surfaces with a lower surface roughness and/or by using higher current densities.

In order to get more insight into the smoothing mechanism, we analyzed the surface roughness by using the spectral
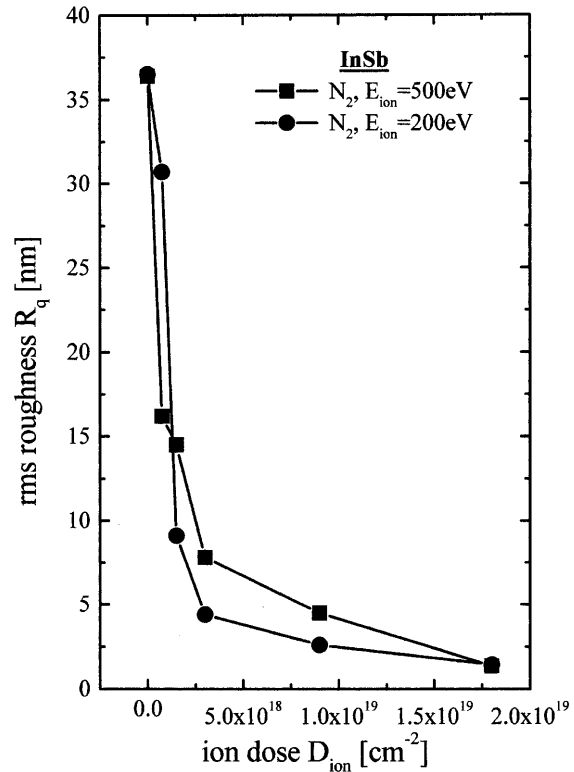

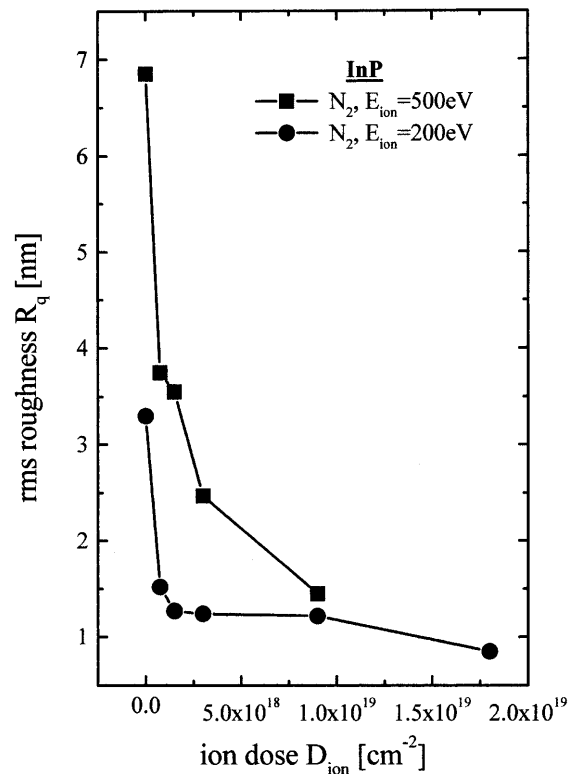**Fig. 5.** Evolution of rms surface roughness of InP as a function of ion dose at two ion beam energies ($E_{\mathrm{ion}} = 200$ eV and $E_{\mathrm{ion}} = 500$ eV) for normal ion beam incidence

power density. The PSD function of different InSb and InP surfaces before and after N_2 ion beam smoothing ($E_{ion} = 200$ eV) has been ploted in Figs. 6 and 7. At this ion beam energy, the etch rates of InP, InSb, and InAs are reduced by a factor of more than 3 compared to those for N_2 RIBE at 500 eV (a more detailed description of the dependence of the etch rates on N_2 RIBE process parameters is given in [7] and [10]). It can be seen that the smoothing of InSb is particularly effective for shorter wavelengths. The same behaviour was observed for InAs. However, the smoothing of the InP surface is not so effective for wavelengths less than about 100 nm (Fig. 7). This is because the N_2 RIBE of InP leads to small spikes spread all over the N_2 etched surface (see Fig. 2b). The existence of such small spikes is characteristic for N_2-RIBE-processed InP surfaces [11]. The smoothing process in this case is reduced because of the existence of these new small surface features, which have a periodicity < 100 nm. We observed that the size of these cones or spikes depends on the ion beam energy, i.e. the size of the cones decreases with decreasing N_2 ion beam energy and hence ion beam smoothing of InP surfaces yields a lower surface roughness at lower ion beam energies (as shown in Fig. 5 for $E_{ion} = 200$ eV and $E_{ion} = 500$ eV).

In contrast to the case for InP, N_2 ion beam smoothing of InSb and InAs surfaces reveals extremely smooth surfaces, almost independent of the ion beam energy in the range investigated. This is not surprising, because we do not observe any influence of the ion beam energy on the surface roughness of initially smooth InAs and InSb surfaces after N_2 RIBE [7], i.e. no differences in the rms surface roughness of the InAs and InSb surfaces can be recognized after N_2 RIBE at $E_{ion} = 200$ eV and $E_{ion} = 500$ eV. We can thus

expect the same final surface roughness for both ion beam energies (see Fig. 4), but it should be mentioned that for smoothing with $E_{ion} = 200$ eV, in comparison to smoothing with $E_{ion} = 500$ eV, less material is removed because of the different etching rates for both energies.

Next the influence of the ion beam angle of incidence on the smoothing process was examined. The results for the ion beam smoothing of the InSb surface (parameters $E_{ion} = 500$ eV and $D_{ion} = 3.0 \times 10^{18}$ cm^{-2}) are represented in Fig. 8, the initial rms value for the InSb surface was about 40 nm. We observed that the process of ion beam smoothing is particularly effective for ion beam angles of incidence smaller than 30° and larger than 70°. For InAs and InP we obtained nearly the same results. Similar results have been published for ion beam smoothing of diamond films with Ar and O_2 [21, 22].

For the discussion of the smoothing mechanism, two points are to be considered. First, the basic condition for ion beam smoothing is that the etching process itself does not cause additional roughness. This condition is fulfilled by the reactive ion beam etching of InAs, InSb, and InP with N_2 [7, 10], with the exception of the small spikes or cones on InP surfaces after N_2 RIBE [11]. Second, for the explanation of the ion beam smoothing process it is necessary to take into account the angle dependence of the etching rate R. It seems reasonable to assume that the maximum etching rate for N_2 RIBE of indium-containing semiconductors is situated within the range between 40° – 50° [10][1]. Furthermore, from the AFM measurements we estimated the bottom angle (α_c), which is defined as the angle between the side and the base of

---

[1] All the binary and ternary indium-containing compound semiconductors we investigated showed a maximum etching rate between 40° and 50°
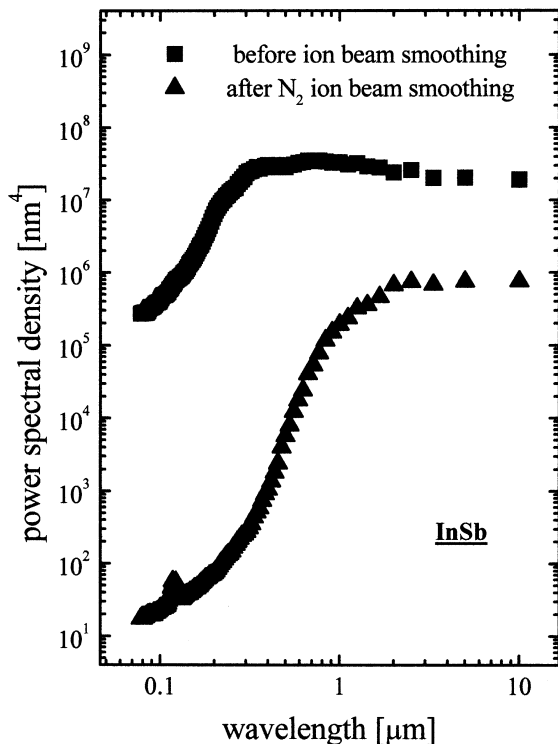

Fig. 6. Power spectral density of the InSb surface before and after N_2 ion beam smoothing with an ion dose of 1.8×10^{19} cm^{-2} ($\alpha_{ion} = 0°$, $E_{ion} = 200$ eV)
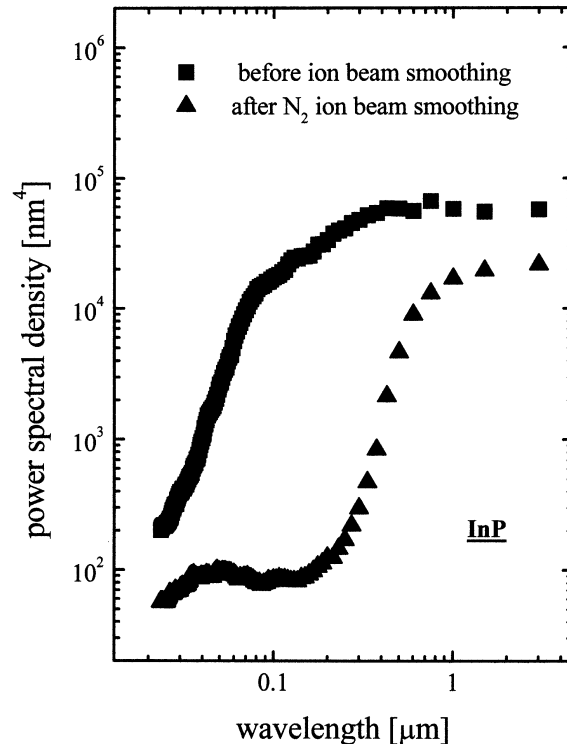

Fig. 7. Power spectral density of the InP surface before and after N_2 ion beam smoothing with an ion dose of 1.8×10^{19} cm^{-2} ($\alpha_{ion} = 0°$, $E_{ion} = 200$ eV)
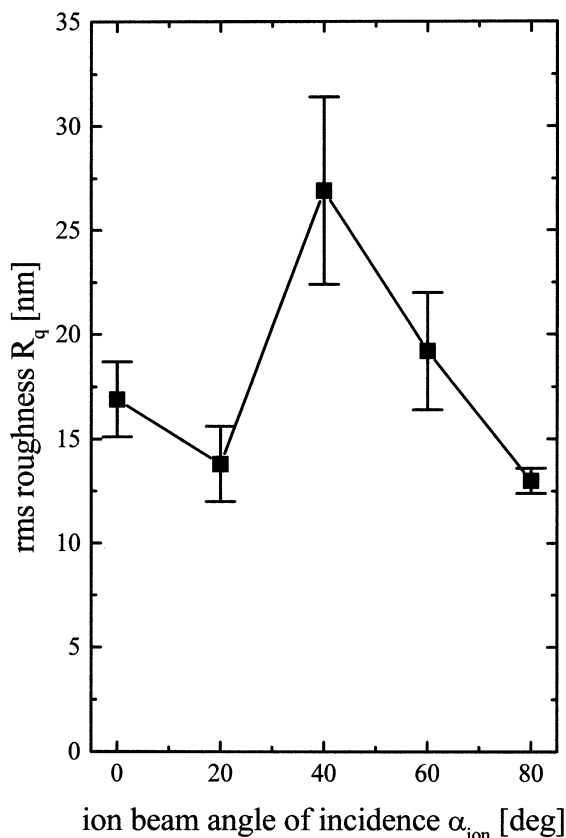
Fig. 8. rms surface roughness of InSb as a function of ion beam incidence angle. The ion beam smoothing was performed with $E_{ion} = 500\,\text{eV}$ and $D_{ion} = 3.0 \times 10^{18}\,\text{cm}^{-2}$

the cones (or in more general, surface features). The largest measured bottom angles were $20°$, $36°$ and about $40° - 60°$ for InAs, InP, and InSb, respectively. Based on these observations, it is now possible to explain the ion beam smoothing by using a simple model, as proposed for ion beam smoothing of diamond films [21]. We will discuss only the smoothing of InSb, because the ion beam smoothing of InP and InAs can be discussed in the same way. We assume that the ion beam angle of incidence is $0°$ and the angle of the side of the cones is $50°$. According to these conditions, the ion beam angle of incidence on the sides of the cones is $50°$. Because the etching rate at an angle of incidence of $50°$ is greater than that at $0°$, the cones are etched faster than the area around the cones, where the ion beam angle of incidence is smaller. Hence, the surface was smoothed with increasing ion dose (or etching depth). At an angle of incidence of $40°$ the ion beam angle of incidence on the sides of the cones is $10°$; because the etching rate at an angle of incidence of $40°$ is greater than that at about $10°$, the cones are etched slower than the area around the cones. Hence, one expects an increased roughness with increasing ion dose (Fig. 8). Surprisingly we can observe this only for ion doses $D_{ion} < 3.0 \times 10^{18}\,\text{cm}^{-2}$ at an ion beam energy of $E_{ion} = 500\,\text{eV}$ or for all ion doses at an ion beam energy of $E_{ion} = 200\,\text{eV}$. This is not yet completely understood. At $80°$, the ion beam angle of incidence on the sides of the cones is now $30°$. Under these conditions the etching rate on the sides of the cones is again larger than around the cones and a smoothing of the surface can be observed. Generally one can say that ion beam smoothing of such cones or surface

features occurs if

$$R(\alpha_i) < R(\alpha_{ci}) < R(\alpha_{max}) , \qquad (1)$$

where R defines the etching rate, α_i is the ion beam angle of incidence around the cones or surface features, α_{ci} is the ion beam angle of incidence on the sides of the cones (given by $\alpha_{ci} = |\alpha_{ion} - \alpha_c|$) and α_{max} is the angle of incidence, where the maximum etching rate occurs. With the help of these considerations it can be understood why smoothing occurs even at angles of incidence close to normal incidence and over $70°$.

It should be mentioned here that this process should be also applicable to other materials for which the conditions specified above (no additional roughness due to the ion beam etching and (1) applies) are fulfilled.

3 Conclusion

We have demonstrated that N_2 reactive ion beam etching can be used to smooth rough surfaces of InAs, InP, and InSb. The ion beam smoothing has been examined as a function of the ion energy, the ion dose and the angle of incidence. We find a drastic improvement in the surface roughness of initially rough surfaces with increasing ion dose at angles of incidence near normal incidence and larger than $70°$. By using this technique, the initial rms roughness of InAs ($R_q = (2.8 \pm 0.1)\,\text{nm}$), InP ($R_q = (3.3 \pm 1.1)\,\text{nm}$), and InSb ($R_q = (36.5 \pm 4.5)\,\text{nm}$) could be reduced to $R_q = (0.2 \pm 0.1)\,\text{nm}$, $R_q = (0.8 \pm 0.1)\,\text{nm}$, and $R_q = (1.4 \pm 0.1)\,\text{nm}$, respectively. The mechanism of ion beam smoothing could be explained by taking into account the angle dependence of the etching rate. The ion beam smooothing should also be applicable to other materials.

References

1. W. Katzschner, A. Steckenborn, R. Löffler, N. Grote: Appl. Phys. Lett. **44**, 352 (1984)
2. O. Wada: J. Phys. D: Appl. Phys. **17**, 2429 (1984)
3. N. Bouadma, P. Delvodere, B. Jusserand, P. Ossart: Appl. Phys. Lett. **44**, 352 (1986)
4. S.J. Pearton, U.K. Chakrabarti, A.P. Perley: J. Appl. Phys. **68**, 2760 (1990)
5. J.B. Malherbe: CRC Crit. Rev. Solid State Mater. Sci. **19**, 55 (1994)
6. C.M. Demanet, J.B. Malherbe, N.G. van der Berg, V. Sankar: Surf. Interface Anal. **23**, 433 (1995)
7. F. Frost, A. Schindler, F. Bigl: Semicond. Sci. Technol. **13**, 523 (1998)
8. S.W. MacLaren, J.E. Baker, N.L. Finnegan, C.M. Loxton: J. Vac. Sci. Technol. A **10**, 468 (1992)
9. L.M. Bharadwaj, P. Bonhomme, J. Faure, G. Balossier, R.P. Bajpai: J. Vac. Sci. Technol. B **9**, 1440 (1991)
10. W. Katzschner, U. Niggebrügge, R. Löffler, H. Schröter–Janssen: Appl. Phys. Lett. **48**, 230 (1986)
11. W. Görtz, B. Kempf, J. Kretz: J. Vac. Sci. Technol. B **13**, 34 (1995)
12. H. Iber, S. Mo, E. Peiner, G. Vollrath, A. Schlachetzki, F. Fiedler: Semicond. Sci. Technol. **12**, 755 (1997)
13. H.W. Dinges, B. Kempf, H. Burkhard, R. Göbel: Appl. Surf. Sci. **50**, 359 (1991)
14. J.M. Bennett, L. Mattsson: *Introduction to Surface Roughness and Scattering* (Optical Society of America, Washington, DC 1989)

15. S.J. Fang, S. Haplepete, W. Chen, C.R. Helms, H. Edwards: J. Appl. Phys. **82**, 5891 (1997)
16. R. Pétri, P. Brault, O. Vatel, D. Henry, E. André, P. Dumas, F. Salvan: J. Appl. Phys. **75**, 7489 (1994)
17. *Nanoscope III, Command Reference Manual* (Digital Instruments, Santa Barbara, CA 1996) version 4.10
18. S. Ilias, G. Sené, P. Möller, V. Stambouli, J. Pascallon, D. Bouchier, A. Gicquel, A. Tardieu, E. Anger, M.F. Ravet: Diamond Relat. Mater. **5**, 835 (1996)
19. E. Chason, T.M. Mayer: Appl. Phys. Lett. **62**, 363 (1993)
20. T.M. Mayer, E. Chason, A.J. Howard: J. Appl. Phys. **76**, 1633 (1994)
21. A. Hirata, H. Tokura, M. Yoshikawa: Thin Solid Films **212**, 43 (1992)
22. S. Kiyohara, I. Miyamoto, T. Masaki, S. Honda: Nucl. Instrum. Methods B **121**, 191 (1997)